Oxygen Atom Reactions with Circumtrindene and Related Molecules: Analogues for the Oxidation of Nanotube Caps

Janice A. Steckel and Kenneth D. Jordan*

Department of Chemistry and Center for Molecular and Materials Simulations, University of Pittsburgh, Pittsburgh, Pennsylvania 15260

Phaedon Avouris

IBM Research Division, T. J. Watson Research Center, Yorktown Heights, New York 10598

Received: December 5, 2001

Circumtrindene, a $C_{36}H_{12}$ open geodesic dome with alternating five- and six-membered rings, is of interest as a vesicle for carrying out chemical reactions and also as a model for certain carbon nanotube caps. Here the addition of an oxygen atom to circumtrindene is examined by means of density functional calculations. O-atom addition to a C−C bond shared between the central and adjacent hexagons gives an epoxide structure while O-atom addition to a C−C bond shared by the central hexagon and an adjacent pentagon results in cleavage of the C−C bond and an R−O−R insertion product. Despite their structural dissimilarity, the two oxidation products are predicted to be of comparable stability (with binding energies of −74.9 and −78.7 kcal/mol, respectively), and to have a large (55.7 kcal/mol) barrier for interconversion.

Introduction

Circumtrindene, (Figure 1a,b), a $C_{36}H_{12}$ geodesic dome comprised of fused five- and six-membered rings, was recently synthesized in high yield by Ansems and Scott.[1] Circumtrindene may be viewed as representing 60% of the C_{60} buckyball, but with the dangling bonds around the perimeter terminated with H atoms. As such, it has the same arrangement of five- and six-membered rings as what is believed to be the most stable cap for the (5,5) armchair and (9,0) zigzag single-walled carbon nanotubes (Figure 1c).[2] Hence, in addition to being of interest in its own right, circumtrindene can be viewed as a model system for understanding the chemical reactivity of carbon nanotube caps. Carbon nanotubes as grown are believed to have capped ends, requiring heat treatment or chemical cutting to yield open-ended tubes.[3−5] Oxidation is one of the commonly used methods for cutting carbon nanotubes.[6,7] It has been shown that oxidation of closed multiwalled nanotubes occurs preferentially at the curved surfaces of the caps,[8−10] and this is believed to also be the case for single-walled nanotubes.[11,12] Thus oxidation opens the tubes, greatly affecting their ability to adsorb chemical species.[13] In addition, oxygen-containing functional groups left behind by oxidative purification and cutting procedures can drastically modify the electronic and other properties of the nanotubes.[7]

In this work we carry out electronic structure calculations to examine the chemical interaction of circumtrindene with oxygen atoms to gain insight into the reactivity of this novel species as well as into the oxidation of carbon nanotube caps. For comparative purposes, we also consider reaction of O atoms with the C_{60} fullerene and corannulene molecules.

* Author to whom correspondence should be addressed.

Computational Methods

The calculations on circumtrindene, C_{60}, corannulene, and their oxides were carried out using density functional theory (DFT)[14] with the Becke3LYP[15] exchange−correlation functional. Minimum energy and transition state structures were optimized without constraints. The nature of key stationary points was ascertained by performing harmonic frequency calculations. Most of the calculations were carried out using the 6-31G(d) basis set.[16] However, the optimization of the transition state for O-atom migration in $C_{60}O$ made use of a mixed basis set treating the oxygen atom and eight nearby carbon atoms with the 6-31G(d) basis set and the remaining carbon atoms with the 3-21G[17] basis set.

To calibrate the reliability of the Becke3LYP functional for characterizing the oxides of circumtrindene and related molecules, the oxides of corannulene were also considered. For this smaller system it was possible to also carry out wave function-based MP2[18] calculations. To gauge the importance of higher-order correlation effects, a smaller model, consisting of two six-membered and two five-membered rings, was constructed (cut out) from the Becke3LYP-optimized circumtrindene and circumtrindene-oxide structures. For this model system, Becke3LYP, MP2 and CCSD(T)[19] single-point energy calculations were carried out. The sensitivity of the results to the basis set was also examined by performing Becke3LYP and MP2 calculations with both the 6-31G(d) and 6-311G(2d)[20] basis sets. All calculations were performed using the Gaussian 98 program.[21]

Results

Oxidation of Circumtrindene. Circumtrindene has C_{3v} symmetry with the central hexagonal ring bounded by alternating pentagons and hexagons. The C−C bonds shared between the central hexagon and adjacent hexagons are designated "6−6",

10.1021/jp014421u CCC: $22.00
Published on Web 02/21/2002

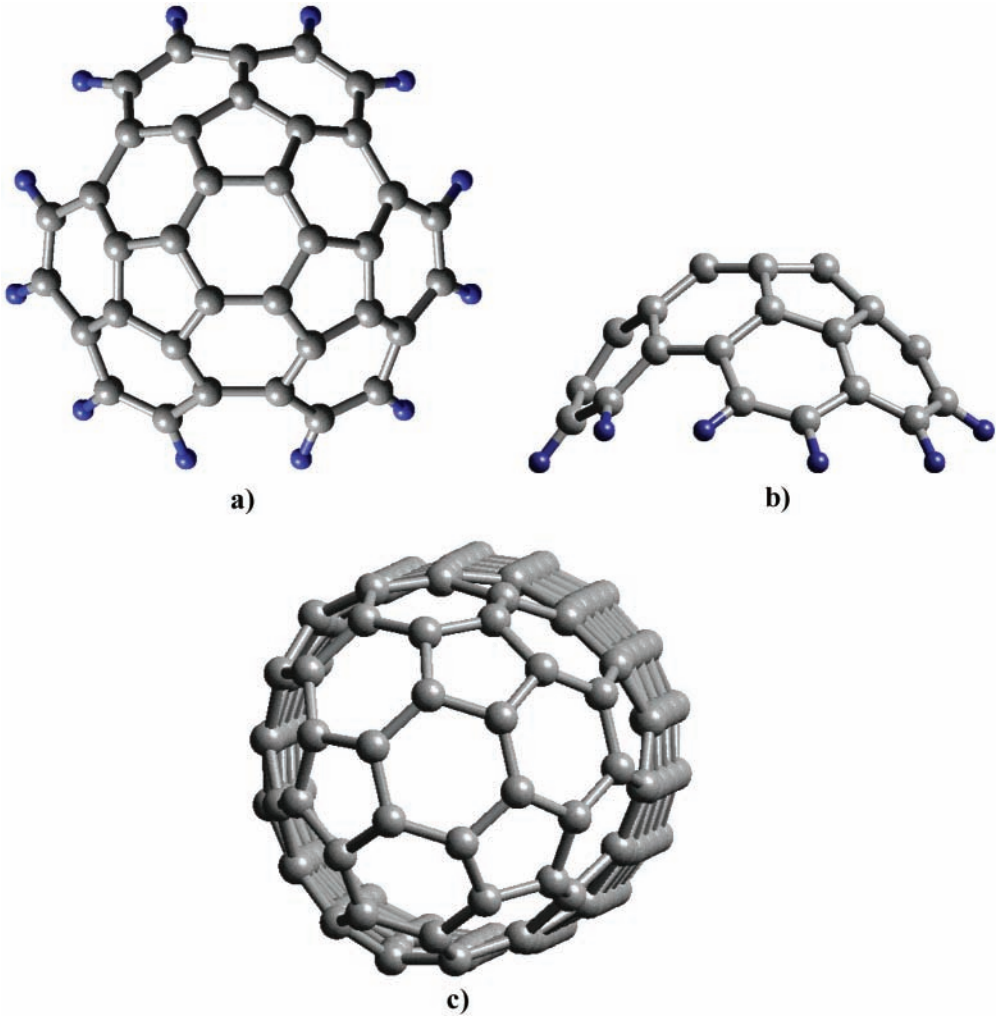

Figure 1. Circumtrindene: top (a) and side (b) views. (9,0) Zigzag nanotube with the most stable cap structure (c).

and those shared between the central hexagon and adjacent pentagons are designated "6−5". The Becke3LYP DFT calculations predict the 6−6 and 6−5 C−C bond lengths to be 1.39 and 1.45 Å, respectively.

In examining the products of O-atom attack on circumtrindene, reactions at both the 6−6 and 6−5 sites and on the inside and outside of the dome were considered. Finally, both spin singlet and triplet states were examined. The calculated binding energies are presented in Table 1. The singlet products formed by O-atom addition on the outside of the dome are described first. Attack at the 6−6 site led to the epoxide structure (Figure 2a), whereas attack at the 6−5 site led to cleavage of the C−C bond and O-atom insertion, to give an R−O−R type product (Figure 2b). (As will be discussed below, an analogous situation has been reported for oxidation of C_{60}.[22])

The two oxide products are of comparable stability, with the binding energies being −74.9 and −78.7 kcal/mol, at the 6−6 and 6−5 sites, respectively. All binding energies are referenced relative to the singlet ground state of the hydrocarbon plus O(^{3}P). Negative binding energies indicate that the binding of the O atom is thermodynamically favored. These binding energies are larger in magnitude than that calculated for epoxide formation at a graphitic surface (−53.1 kcal/mol) but are comparable to that calculated for epoxide formation at the outer wall of a (8,0) single-walled carbon nanotube.[23] Calculation of the vibrational frequencies in the harmonic approximation confirms that both of these oxidation products of circumtrindene are indeed local minima on the potential energy surface.

TABLE 1: Calculated Binding Energies for Products of Oxygen Atom Attack on Circumtrindene, C_{60}, and Corranulene[a]

			binding energy (kcal/mol)	
	site of attack	species	Becke3LYP	MP2
circumtrindene	6−6 site, outside	singlet	−74.9	
		triplet	−29.0	
	6−6 site, inside	singlet	15.2	
		triplet	49.8	
	6−5 site, outside	singlet	−78.7	
		triplet	−34.9	
	6−5 site, inside	singlet	32.4	
		triplet	38.4	
	on-top, outside	triplet	−32.5	
C_{60}	6−6 site, outside	singlet	−76.4	
	6−5 site, outside	singlet	−78.5	
corannulene	6−6 site, outside	singlet	−55.9	−55.0
	6−5 site, outside	singlet	−61.4	−59.7

[a] All results obtained using the 6-31G(d) basis set.

With the exception of the 6−5 inside site, the triplet oxidation products are much less stable than their singlet counterparts. The binding energies of the triplet oxidation products formed by attack at the 6−6 and 6−5 sites of the outside of the circumtrindene molecule are predicted to be −29.0 and −34.9 kcal/mol, respectively, at the Becke3LYP/6-31G(d) level. The calculations also revealed a spin triplet product with the O atom on the outside of the dome, directly above a carbon of the central

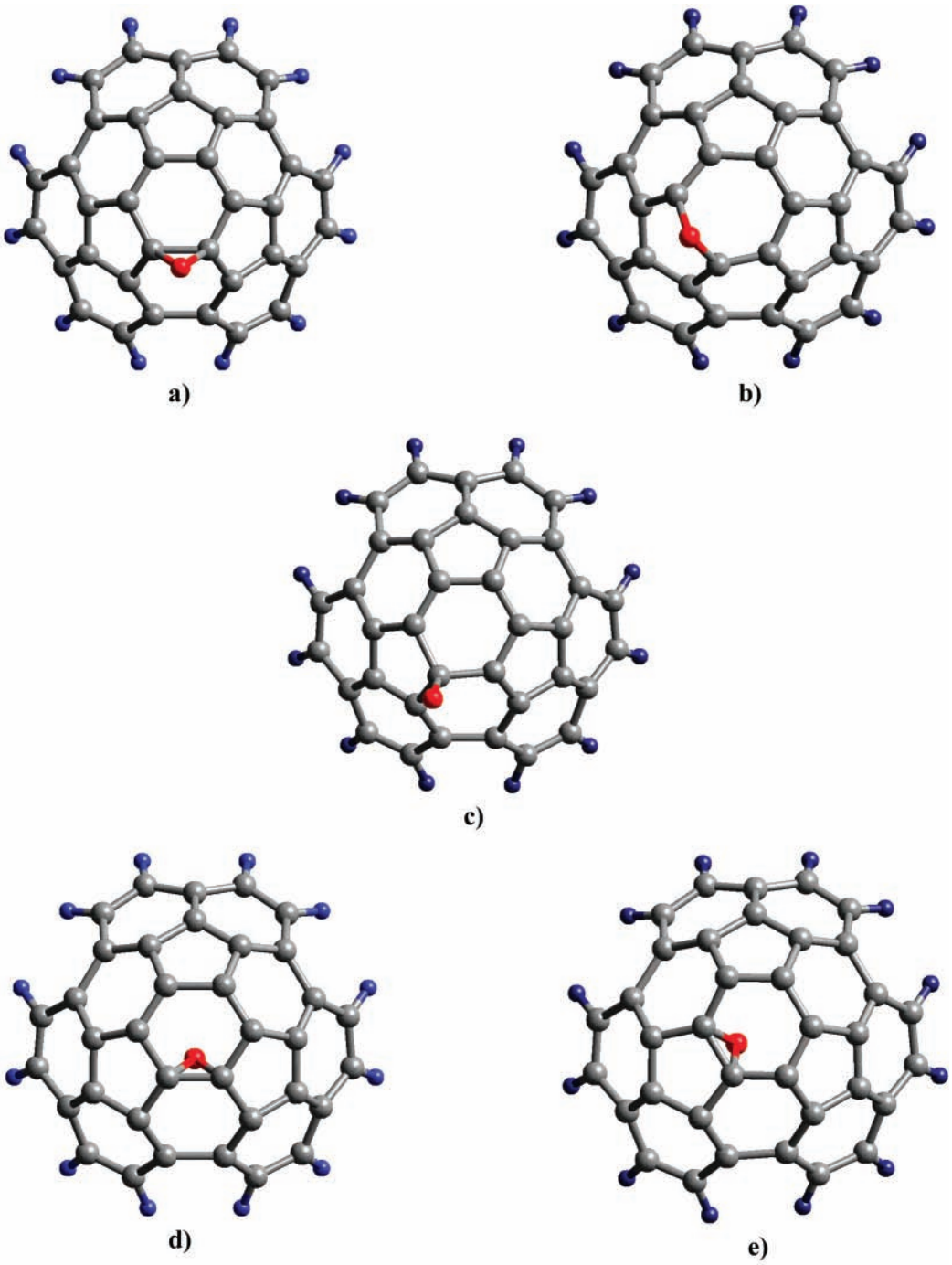

Figure 2. Adducts of attack by oxygen on circumtrindene. Attack at the 6−6 bond from the outside, epoxide product (a); attack at the 6−5 bond from the outside, R−O−R product (b); attack at the central hexagon, "on-top" triplet product (c); attack at the 6−6 bond from the inside, epoxide product (d); attack at the 6−5 bond from the inside, epoxide product (e).

hexagon (Figure 2c). This species is calculated to be bound by −32.5 kcal/mol, which is similar in stability to the external epoxide and R−O−R triplet products.

O-atom attack at both 6−6 and 6−5 sites on the inside of the circumtrindene dome leads to epoxide products (Figures 2d and 2e). However the formation of these species, both singlet and triplet, is predicted to be endothermic.

Comparison with Oxides of C_{60}. The finding that O-atom attack at the 6−6 and 6−5 sites of circumtrindene gives epoxide and R−O−R structures, respectively, is reminiscent of the situation for C_{60}, for which Raghavachari and Sosa predicted an epoxide product for O-atom attack at the 6−6 bond and an R−O−R product for attack at the 5−6 bond.[22,24] Both isomers of $C_{60}O$ have been observed experimentally.[25,26] In their theoretical investigation of C_{60}, Raghavachari and Sosa used the semiempirical MNDO,[27] local density DFT, and Hartree−Fock methods.

To facilitate comparison with our results for circumtrindene, we have optimized the geometry of C_{60} and of the two $C_{60}O$ isomers at the Becke3LYP/6-31G(d) level of theory. The optimized structures of the oxide species are shown in Figure 3, and the associated binding energies are listed in Table 1. In agreement with Raghavachari and Sosa, we find that attack at a 6−6 bond gives an epoxide product, while attack at a 6−5 bond gives an R−O−R insertion product. As seen from Table 1, the O-atom binding energies for the two $C_{60}O$ isomers are

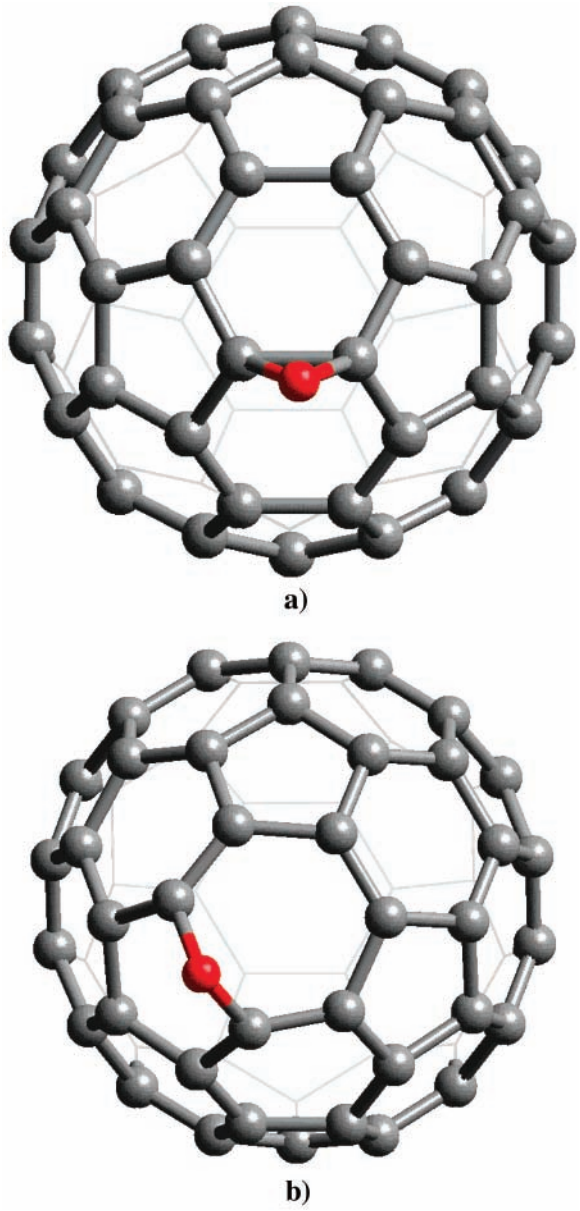

Figure 3. Adducts of attack by oxygen at 6−6 and 6−5 bonds of C_{60}. Attack at the 6−6 bond, epoxide product (a); attack at the 6−5 bond, R−O−R product (b).

similar to those in the analogous circumtrindene oxides. Additionally, the structures (i.e., key C−C and C−O distances, presented in Table 2) of the $C_{60}O$ oxides differ only slightly from those of the analogous circumtrindene oxides.

Rearrangement Pathways of the Oxides of Circumtrindene and C_{60}. The transition states for the rearrangement between the singlet R−O−R and epoxide isomers of circumtrindene and C_{60} were optimized using the Becke3LYP functional. In the case of the circumtrindene oxide system, the 6-31G(d) basis set was used. For the larger $C_{60}O$ system, the 6-31G(d) basis set was used only for the O atom and eight nearby carbon atoms (see Figure 4) and the remaining carbon atoms were described with the 3-21G basis set. For the purpose of calculating the activation energies, the R−O−R oxide and epoxide species of C_{60} were reoptimized using the mixed basis set.

In the transition state structure for both circumtrindene oxide and $C_{60}O$, the oxygen atom is located above a carbon atom that is common to the 6−5 and 6−6 bonds. The transition state for the circumtrindene oxide rearrangement is shown in Figure 5.

TABLE 2: Calculated Geometrical Parameters of the Oxides of Circumtrindene, C_{60}, and Corannulene[a]

		bond lengths (Å)[b]		
	species	6−5 C−C	6−6 C−C	C−O
circumtrindene	R−O−R	2.12	1.37	1.40
	TS	1.52	1.49	1.37
	epoxide	1.48	1.53	1.42
C_{60}	R−O−R	2.14	1.38	1.38
	TS	1.56	1.52	1.35
	epoxide	1.49	1.53	1.42
corannulene	R−O−R	2.08 (2.06)	1.38 (1.39)	1.38 (1.39)
	TS	1.49 (1.47)	1.50 (1.48)	1.37 (1.40)
	epoxide	1.47 (1.46)	1.51 (1.51)	1.41, 1.47 (1.42, 1.48)

[a] Results in parentheses from MP2/6-31G(d) optimizations. All other results were obtained from Becke3LYP optimizations. A mixed 6-31G(d)/3-21G basis set was used for $C_{60}O$; the 6-31G(d) basis set was used for the circumtrindene and corannulene oxides. [b] The 6−5 and 6−6 C−C bonds separate a hexagon from an adjacent pentagon or hexagon, respectively, as described in the text. In the R−O−R adduct, the first distance reported is that between the two carbons formerly joined by the 6−5 bond. The two C−O bonds in the 6−6 oxide of corannulene are unequal.

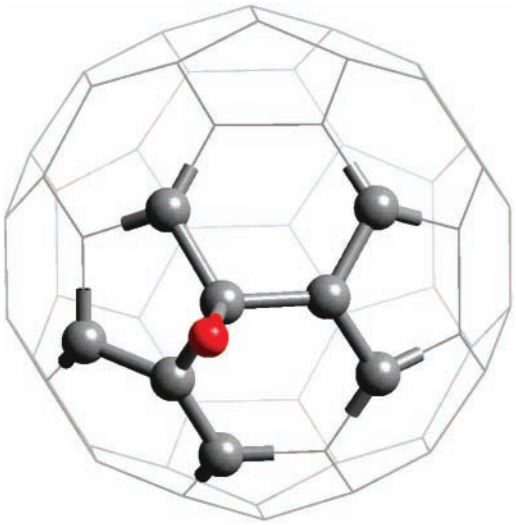

Figure 4. Specification of the mixed basis set used for optimization of the transition state and minimum energy structures of $C_{60}O$ in the calculation of the activation energy. The oxygen atom and the eight carbon atoms described with the 6-31G(d) basis set are depicted as spheres; the remaining carbon atoms were described with the 3-21G basis set.

The key geometrical parameters as well as the activation and reaction energies are summarized in Tables 2 and 3. The activation energy for rearrangement from the 6−5 to the 6−6 oxide of circumtrindene is calculated to be 55.7 kcal/mol and that for the rearrangement from the 6−5 to the 6−6 form of $C_{60}O$ is calculated to be 52.8 kcal/mol.

Raghavachari and Sosa reported that MNDO-level calculations of the reaction path for interconversion between the two $C_{60}O$ isomers gave a stable "on top" intermediate structure with the oxygen atom located above the carbon atom that is shared by the 6−6 and 6−5 bonds. This intermediate was calculated to be about 60 kcal/mol higher in energy than the epoxide and R−O−R species. Using the MNDO method, we located "on top" intermediates for both $C_{60}O$ and circumtrindene oxide systems. However, in both cases, a Beck3LYP optimization starting from the MNDO-optimized geometry of the intermediate relaxed to the 6−6 epoxide species. In the case of circumtrindene, we also carried out transition state optimizations using

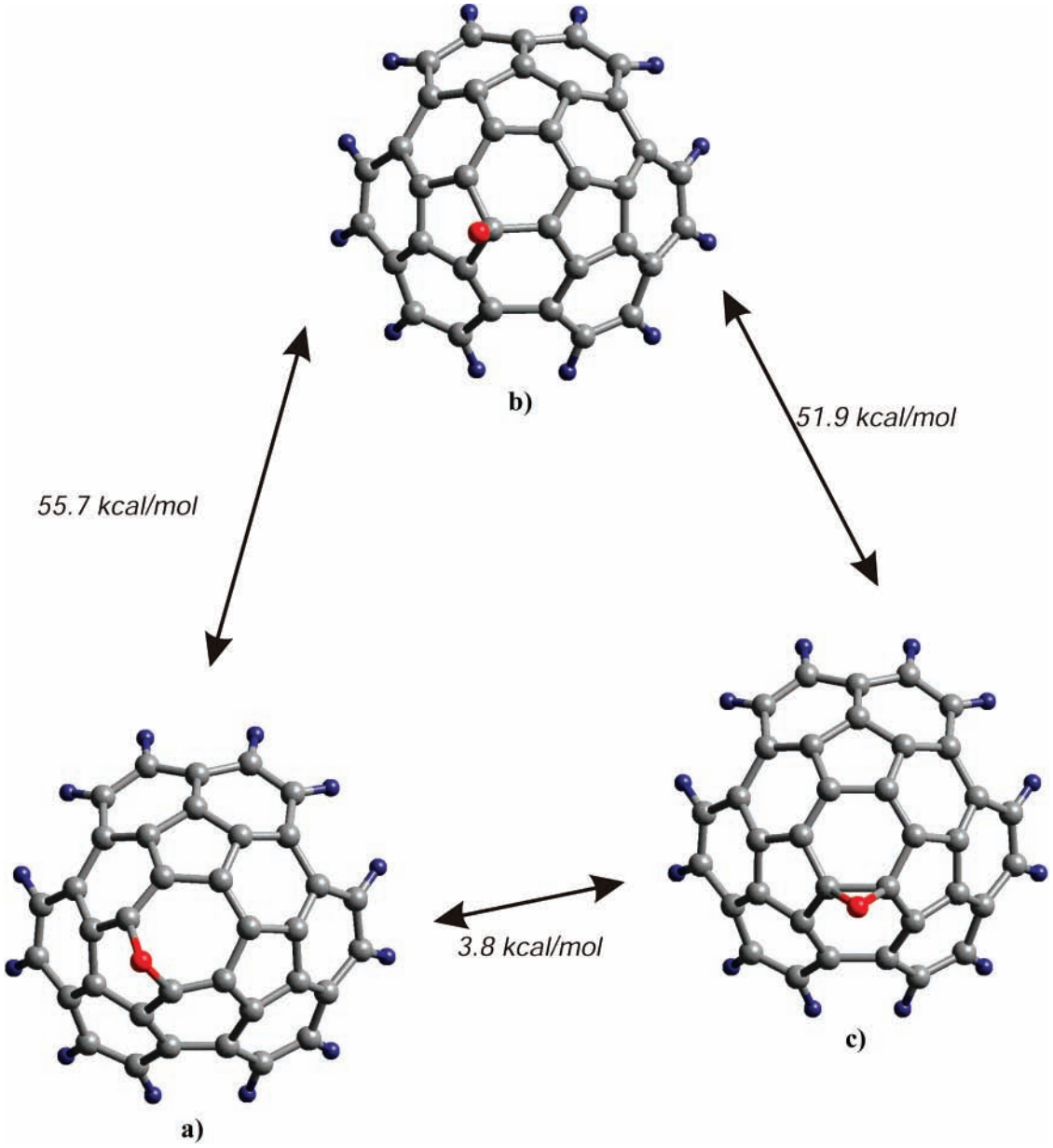

Figure 5. Rearrangement between the two oxides of circumtrindene. 6−5 R−O−R isomer (a); transition state (b); 6−6 epoxide isomer (c).

TABLE 3: Calculated Energy Differences (kcal/mol) for Rearrangements between Oxides of Circumtrindene, C_{60}, and Coranulene[a]

	barrier height		reaction energy	
	Becke3LYP	MP2	Becke3LYP	MP2
circumtrindene	55.7	-	3.8	-
C_{60}	52.8[b]	-	2.1	-
corannulene	42.6	54.2	5.5	4.7

[a] The activation barrier and reaction energies are given for rearrangement from the R−O−R oxide to the epoxide. [b] A mixed 6-31G(d)/3-21G basis set as described in the text was used for calculating the $C_{60}O$ reaction barrier; the 6-31G(d) basis set was used for calculating the other energy differences.

the Becke3LYP functional starting from the two distinct transition states located using the MNDO method. These optimizations both converged at the single circumtrindene oxide transition state described above. We conclude therefore that the prediction of two transition states and a stable "on-top" intermediate in the 6−5 to 6−6 rearrangement for circumtrindene oxide and for $C_{60}O$ is an artifact of the MNDO method.

Calibration of the DFT Results. To establish the reliability of the Becke3LYP method for describing the oxidation of circumtrindene and related molecules, it is desirable to carry out high-level, wave function-based calculations. However, for the circumtrindene oxides and $C_{60}O$ species, MP2 or higher-level calculations would be computationally prohibitive. For this reason we have considered corannulene, a dome-shaped polycyclic aromatic molecule consisting of a central pentagon surrounded by six hexagons and terminated at the edges by hydrogen atoms. Thus, in common with circumtrindene and C_{60}, corannulene possesses both 6−6 and 6−5 sites, making it an ideal test system for establishing the reliability of density functional methods for describing O-atom interactions at these sites. Products of O-atom attack at the 6−6 and 6−5 sites of corannulene as well as the transition state for the rearrangement between the oxides were optimized using the Becke3LYP and MP2 procedures with the 6-31G(d) basis set. From the geometrical parameters indicated in Figure 6, it is seen that the two methods give similar geometrical structures. Moreover, the geometrical parameters for the corannulene oxide system are

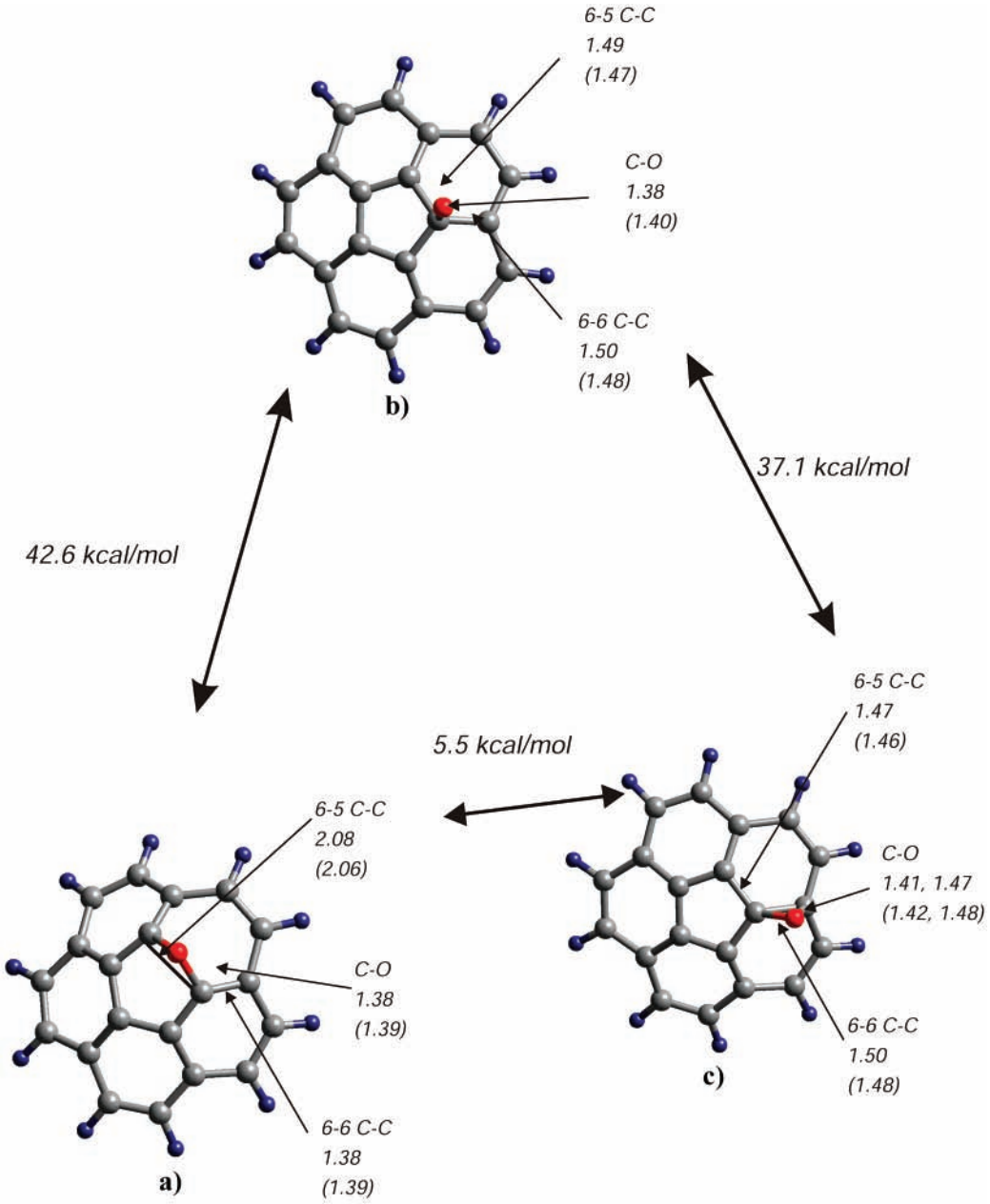

Figure 6. Rearrangement between the two oxides of corannulene. 6−5 R−O−R isomer (a); transition state (b); 6−6 epoxide isomer (c). The energies differences are from Becke3LYP calculations. Both Becke3LYP and MP2 bond lengths (in Å) are reported, with the latter being given in parentheses.

similar to those obtained for $C_{60}O$ and the circumtrindene oxides, as may be seen from the results reported in Table 2. This supports the use of corannulene as a test system for the reliability of theoretical methods for describing the interaction of O atoms with the larger C_{60} and circumtrindene molecules.

The binding energies for the oxidation products and the energy differences for rearrangements between the oxides of corannulene are reported in Tables 1 and 3. For the corannulene test system, the Becke3LYP binding energies differ by less than 2 kcal/mol from the MP2 values. On the other hand, the Becke3LYP method gives an activation energy for the R−O−R → epoxide rearrangement 11.6 kcal/mol lower than the MP2 value. As will be shown below, the MP2 method overestimates the activation energy for such rearrangement processes.

The good agreement between the Becke3LYP and MP2 O-atom energy differences and geometrical parameters for corannulene suggests that the Becke3LYP functional is well suited for describing O-atom reactions with corannulene, circumtrindene, and related systems. However, to establish this conclusively, it is necessary to consider the sensitivity of the results to the inclusion of higher-order correlation effects, e.g., by means of the coupled-cluster CCSD(T) method and the use of more flexible basis sets. Large basis set CCSD(T) calculations would be computationally prohibitive even for corannulene, and instead we carried out such calculations for O-atom reactions with a model for the part of the circumtrindene molecule involved in the O-atom interaction. Specifically, using the Becke3LYP/6-31G(d) geometry of circumtrindene, we cut out a portion of the molecule consisting of two hexagonal and two pentagonal rings, with the dangling bonds being saturated with hydrogen atoms. The CCH angles of the terminating H atoms were chosen to match the corresponding CCC angles of circumtrindene, and the CH bond lengths were taken to be 1.06 Å. The resulting model compound, shown in Figure 7, is a

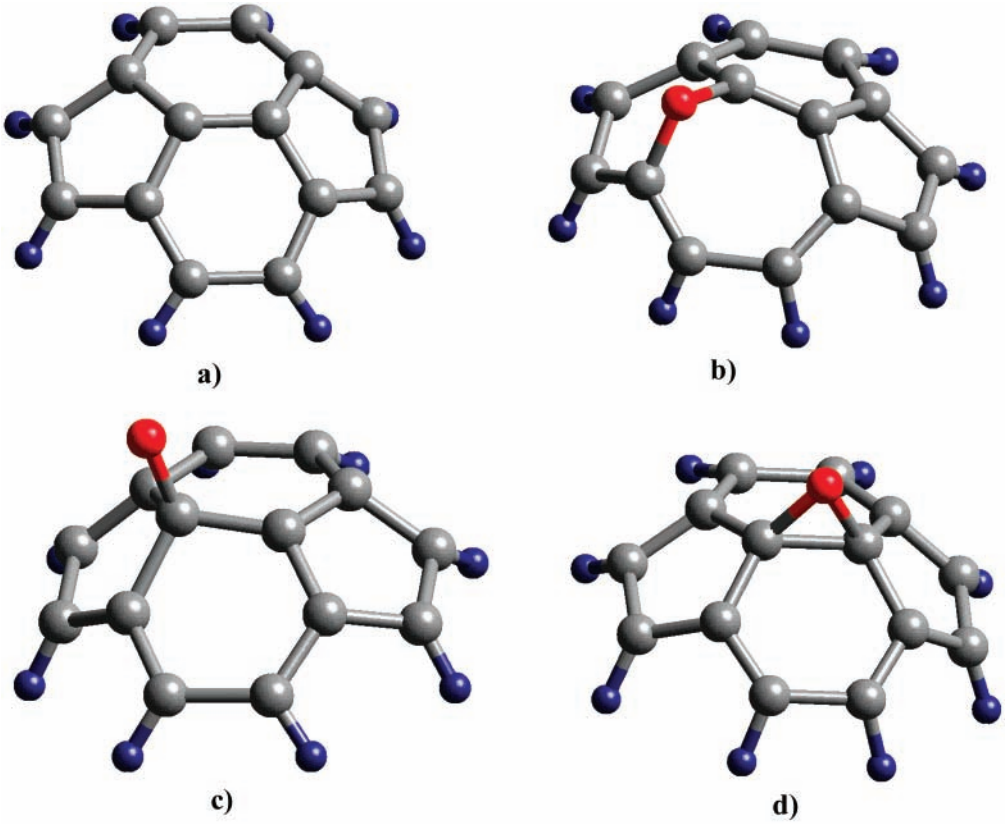

Figure 7. Model used for the coupled cluster calculations. This distorted version of the pyracylene molecule ($C_{14}H_8$) has the geometrical parameters of the Becke3LYP/6-31G(d) optimized circumtrindene molecule, as described in the text. $C_{14}H_8$ model (a); 6−5 R−O−R isomer (b); transition state (c); 6−6 epoxide isomer (d).

TABLE 4: Calculated Energy Differences for Oxygen Attack at the 6−5 and 6−6 Bonds of Distorted Pyracylene and for Rearrangement between the Oxides[a]

	binding energy (kcal/mol)		reaction and activation energies(kcal/mol)	
theoretical method	6−5 site	6−6 site	barrier	reaction
Becke3LYP/6-31G(d)	−75.7	−70.8	45.8	4.9
Becke3LYP/6-311G(2d)	−74.3	−68.4	44.4	5.9
MP2/6-31G(d)	−70.3	−67.5	54.1	2.8
MP2/6-311G(2d)	−74.1	−69.1	53.8	5.0
CCSD(T)/6-31G(d)	−65.7	−63.3	48.1	2.4
CCSD(T)/6-311G(2d)[b]	−69.5	−64.9	47.8	4.6

[a] Single-point calculations performed on distorted pyracylene and pyracylene oxide models generated from the Becke3LYP/6-31G(d) optimized geometry of circumtrindene and its oxide as described in the text. [b] The CCSD(T)/6-311G(2d) results were estimated by correcting the energies obtained at the CCSD(T)/6-31G(d) level of theory with the energy changes found in going from the MP2/6-31G(d) to the MP2/6-311G(2d) procedure.

distorted pyracylene molecule ($C_{14}H_8$). An analogous procedure was followed for the R−O−R, 6−6 epoxide, and transition state structures of circumtrindene. Single-point energy calculations using the Becke3LYP and MP2 methods were performed on the distorted pyracylene and pyracylene oxide models with both the 6-31G(d) and 6-311G(2d) basis sets. In addition, CCSD(T) calculations were carried out using the 6-31G(d) basis set. CCSD(T)/6-311G(2d) results were estimated using a G2-like[28] approach, namely: the difference between the MP2/6-31G(d) and MP2/6-311G(2d) energies was applied as a correction to the CCSD(T)/6-31G(d) energies. The results are presented in Table 4.

The calculations on the distorted pyracylene model system show that expansion of the basis set from 6-31G(d) to 6-311G(2d) leads to a 1.4−2.4 kcal/mol reduction in magnitude in the DFT binding energies and a 1.6−3.8 kcal/mol increase in magnitude in the MP2 binding energies. However, the changes in the reaction and activation energies accompanying this basis set expansion are smaller, being 1.4 kcal/mol or less in the DFT calculations and 2.2 kcal/mol or less in the MP2 calculations. The changes due to inclusion of high-order correlation effects (i.e., in going from MP2 to CCSD(T)) are more important, with the binding energies decreasing in magnitude by 4.2 and 4.6 kcal/mol at the 6−5 and 6−6 sites, respectively, and the activation energy decreasing by 6.0 kcal/mol.

From Table 4 it is seen that the Becke3LYP/6-311G(2d) values of the reaction and activation energies are in good agreement (i.e., within 3.5 kcal/mol) with the CCSD(T)/6-311G(2d) estimates of these quantities, providing justification for the use of the Becke3LYP procedure for characterizing the oxides of circumtrindene and C_{60}.

Discussion

The family of open geodesic polyarene molecules has generated a great deal of interest.[29−32] While a large number of fullerene fragments have been synthesized and characterized by various means, much remains to be discovered about their structure and chemical reactivity. Circumtrindene, studied here, has three different types of 6−6 bonds, with differing degrees of pyramidalization. Scott et al. have reported a strong regioselectivity for attack at the strained 6−6 bonds near the center of the circumtrindene molecule.[30] This type of regioselectivity is also seen in the fullerene, C_{70}.[33]

In the present work, we have considered the reactivity of the C−C bonds near the center of the circumtrindene molecule

toward O atoms. Our calculations predict the existence of nearly isoenergetic 6−6 epoxide and 6−5 insertion products. At first sight, the comparable stability of the two oxidation products is surprising. We believe it can be rationalized as follows: in the dominant valence-bond structure, the 6−6 sites are doubly bonded and the 6−5 sites are singly bonded, so that, roughly speaking, formation of an epoxide at a 6−6 site or of an R−O−R species at a 6−5 site both involve the loss of one C−C bond and the formation of two C−O bonds. A relatively high barrier is calculated for interconversion between the two oxidation adducts, indicating that it should be possible to observe both adducts experimentally. Indeed, both the 6−5 and 6−6 oxides have been observed for $C_{60}O$.

As discussed in the Introduction, the oxidation of single-walled carbon nanotubes is expected to occur preferentially at wall defects and at the caps. Since circumtrindene has a bonding arrangement similar to that of certain carbon nanotube caps, our results are also relevant to the problem of oxidation of the caps. Although isolated O atoms are generally not used in nanotube oxidation, ozone, which has been found to have similar reactivity,[25] is used for this purpose.

Conclusions

Density functional theory has been used to characterize the products of O-atom attack on circumtrindene, C_{60}, and corannulene. For circumtrindene, attack at the 6−6 site on the outside of the dome led to an epoxide structure while attack at the 6−5 site led to an R−O−R insertion structure. These products are very stable, with Becke3LYP/6-31G(d) binding energies of −74.9 and −78.7 kcal/mol, respectively. Adducts of O-atom attack at the inside of the dome are predicted to be significantly less stable with positive binding energies and the triplet oxidation products are calculated to be less stable than their singlet counterparts. O-atom attack at the (outer) 6−6 and 6−5 sites of C_{60} and corannulene lead to adducts with binding energies and geometrical parameters that are similar to their counterparts in the circumtrindene system. Large energy barriers are predicted for rearrangement between the R−O−R and epoxide products for the circumtrindene oxide, $C_{60}O$ and corannulene oxide systems; for circumtrindene this barrier is 55.7 kcal/mol.

Acknowledgment. The calculations were carried out on the IBM 43P computer cluster in the Center for Molecular and Materials Simulations. These computers were funded by the NSF and IBM. J. A. Steckel acknowledges fellowship support from the Lubrizol Corporation.

References and Notes

(1) Ansems, R. B. M.; Scott, L. T. *J. Am. Chem. Soc*. **2000**, *122*, 2719.

(2) Brinkmann, G.; Fowler, P. W.; Manolopoulos, D. E.; Palser, A. H. R. *Chem. Phys. Lett.* **1999**, *315*, 335.

(3) Liu, J.; Rinzler, A. G.; Dai, H.; Hafner, J. H.; Bradley, R. K.; Boul, P. J.; Lu, A.; Iverson, T.; Shelimov, K.; Huffman, C. B.; Rodriguez-Macias, F.; Shon, Y.; Lee, T. R.; Colbert, D. T.; Smalley, R. E. *Science* **1998**, *280*, 1253.

(4) Kuznetsova, A.; Mawhinney, D. B.; Naumenko, V.; Yates, J. T., Jr.; Liu, J.; Smalley, R. E. *Chem. Phys. Lett.* **2000**, *321*, 292.

(5) Fujiwara, A.; Ishii, K.; Suematsu, H.; Kataura, H.; Maniwa, Y.; Suzuki, S.; Achiba, Y. *Chem. Phys. Lett.* **2001**, *336*, 205.

(6) Mawhinney, D. B.; Naumenko, V.; Kuznetsova, A.; Yates, J. T., Jr. *J. Am. Chem. Soc.* **2000**, *122*, 2383.

(7) Collens, P. G.; Bradley, K.; Ishigami, M.; Zettl, A. *Science* **2000**, *287*, 1801.

(8) Ajayan, P. M.; Ebbesen, T. W.; Ichihashi, T.; Iijima, S.; Tanigaki, K.; Hiura, H. *Nature* **1993**, *362*, 522.

(9) Tsang, S. C.; Harris, P. J. F.; Green, M. L. H. *Nature* **1993**, *362*, 520.

(10) Ajayan, P. M.; Iijima, S. *Nature* **1993**, *361*, 333.

(11) Dillon, A. C.; Jones, K. M.; Bekkedahl, T. A.; Kiang, C. H.; Bethune, D. S.; Heben, M. J. *Nature* **1997**, *386*, 377.

(12) Mazzoni, M. S. C.; Chacham, H.; Ordejón, P.; Sánchez-Portal, D.; Soler, J. M.; Artacho, E. *Phys. Rev. B* **1999**, *60*, 2208.

(13) Kuznetsova, A.; Yates, J. T., Jr.; Liu, J.; Smalley, R. E. *J. Chem. Phys.* **2000**, *112*, 9590.

(14) (a) Hohenberg, P.; Kohn, W. *Phys. Rev. B* **1964**, *136*, 864. (b) Kohn, W.; Sham, L. J. *Phys. Rev. A* **1965**, *140*, 1133.

(15) The Becke3LYP functional combines Becke's 1993 exchange functional (Becke, A. D.; *J. Chem. Phys.* **1993**, *98*, 5648) and the correlation functional of Lee, Yang, and Parr (Lee, C.; Yang, W.; Parr, R. G. *Phys. Rev. B* **1988**, *37*, 785).

(16) (a) Hehre, W. J.; Ditchfield, R.; Pople, J. A. *J. Chem. Phys.* **1972**, *56*, 2257. (b) Gordon, M. S. *Chem. Phys. Lett.* **1980**, *76*, 163. (c) Hariharan, P. C.; Pople, J. A. *Theor. Chim. Acta* **1973**, *28*, 213.

(17) (a) Binkley, J. S.; Pople, J. A.; Hehre, W. J. *J. Am. Chem. Soc.* **1980**, *102*, 939. (b) Pietro, W. J.; Francl, M. M.; Hehre, W. J.; Defrees, D. J.; Pople, J. A.; Binkley, J. S. *J. Am. Chem. Soc.* **1982**, *104*, 5039. (c) Dobbs, K. D.; Hehre, W. J. *J. Comput. Chem*. **1986**, *7*, 359. (d) Dobbs, K. D.; Hehre, W. J. *J. Comput. Chem*. **1987**, *8*, 861.

(18) Møller, C.; Plesset, M. S. *Phys. Rev.* **1934**, *46*, 618.

(19) Pople, J. A.; Krishnan, R.; Schlegel, H. B.; Binkley, J. S. *Int. J. Quantum Chem.* **1978**, *14*, 545.

(20) (a) Binning, R. C., Jr.; Curtiss, L. A. *J. Comput. Chem.* **1990**, *11*, 1206. (b) McGrath, M. P.; Radom, L. *J. Chem. Phys.* **1991**, *94*, 511. (c) Curtiss, L. A.; McGrath, M. P.; Blaudeau, J.-P.; Davis, N. E.; Binning, R. C., Jr.; Radom, L. *J. Chem. Phys.* **1995**, *103*, 6104.

(21) Frisch, M. J.; Trucks, G. W.; Schlegel, H. B.; Scuseria, G. E.; Robb, M. A.; Cheeseman, J. R.; Zakrzewski, V. G.; Montgomery, J. A., Jr.; Stratmann, R. E.; Burant, J. C.; Dapprich, S.; Millam, J. M.; Daniels, A. D.; Kudin, K. N.; Strain, M. C.; Farkas, O.; Tomasi, J.; Barone, V.; Cossi, M.; Cammi, R.; Mennucci, B.; Pomelli, C.; Adamo, C.; Clifford, S.; Ochterski, J.; Petersson, G. A.; Ayala, P. Y.; Cui, Q.; Morokuma, K.; Malick, D. K.; Rabuck, A. D.; Raghavachari, K.; Foresman, J. B.; Cioslowski, J.; Ortiz, J. V.; Baboul, A. G.; Stefanov, B. B.; Liu, G.; Liashenko, A.; Piskorz, P.; Komaromi, I.; Gomperts, R.; Martin, R. L.; Fox, D. J.; Keith, T.; Al-Laham, M. A.; Peng, C. Y.; Nanayakkara, A.; Challacombe, M.; Gill, P. M. W.; Johnson, B.; Chen, W.; Wong, M. W.; Andres, J. L.; Gonzalez, C.; Head-Gordon, M.; Replogle, E. S.; Pople, J. A. *Gaussian 98* (Revision A.9); Gaussian, Inc.: Pittsburgh, PA, 1998.

(22) Raghavachari, K. *Chem. Phys. Lett*. **1992**, *195*, 221.

(23) Sorescu, D. C.; Jordan, K. D.; Avouris, Ph. *J. Phys. Chem. B* **2001**, *105*, 11227.

(24) Raghavachari, K.; Sosa, C. *Chem. Phys. Lett.* **1993**, *209*, 223.

(25) He, H.; Swami, N.; Koel, B. E. *J. Chem. Phys.* **1999**, *110*, 1173.

(26) Creegan, K. M.; Robbins, J. L.; Robbins, W. K.; Millar, J. M.; Sherwood, R. D.; Tindall, P. J.; Cox, D. M. *J. Am. Chem. Soc.*, **1992**, *114*, 1103.

(27) Dewar, M. J. S.; Thiel, W. *J. Am. Chem. Soc.* **1977**, *99*, 4899.

(28) Curtiss, L. A.; Raghavachari, K.; Pople, J. A. *J. Chem. Phys.* **1993**, *98*, 1293.

(29) Rabideau, P. W.; Sygula, A. *Acc. Chem. Res.* **1996**, *29*, 235.

(30) Scott, L. T.; Bronstein, H. E.; Preda, D. V.; Ansems, R. B. M.; Bratcher, M. S.; Hagen, S. *Pure Appl. Chem.* **1999**, *71*, 209.

(31) Preda, D. V.; Scott, L. T. *Tetrahedron Lett.* **2000**, *41*, 9633.

(32) Klärner, F.-G.; Panitzky, J.; Preda, D.; Scott, L. T. *J. Mol. Model.* **2000**, *6*, 318.

(33) Hawkins, J. M.; Meyer, A.; Solow, M. A. *J. Am. Chem. Soc.* **1993**, *115*, 7499.